An instrumented reverse-anatomy shoulder prosthesis for assessing the effect of rotator cuff degeneration on glenohumeral joint force *in vivo*.

Stephen JG Taylor, Gordon W Blunn, Ian L Bayley*, Simon M Lambert*. Centre for Biomedical Engineering, Institute of Orthopaedics and Musculoskeletal Science, University College London, Stanmore HA7 4LP; *Royal National Orthopaedic Hospital, Brockley Hill, Stanmore HA7 4LP, UK.

SYNOPSIS

Although the number of patients with rotator cuff (RC) arthropathy presenting for treatment is increasing, there is little knowledge of the muscle activity required to undertake certain everyday tasks or the resulting joint and muscle forces. Rotator cuff degeneration occurs to varying degrees clinically, but no correlation with muscle or joint forces is available. The pattern of force transfer across the joints of shoulder replacement patients with RC deficiency will determine the optimum design of implant which gives them best freedom of movement but maintains stability. In order to correlate rotator cuff degeneration with joint force profile over a range of everyday activities, patients having a range of RC deficiency are being selected to receive an instrumented glenoid implant instead of a normal Bayley-Walker reverse-anatomy implant normally used in these cases. This paper will present the structure, function and testing of the modified implant, the calibration procedure and a comparison of measured strain sensitivities for applied forces with those predicted from a finite element model.

1. INTRODUCTION

1.1 Clinical Significance

The number of patients with rotator cuff (RC) arthropathy presenting for treatment is increasing. However, the failure of conventional Total Shoulder Replacement (TSR), and hemi-arthroplasty, to provide a durable solution in patients with RC deficiency has resurged interest in reverse anatomy prostheses, exemplified in recent times by the increasingly widespread use of the Delta prostheses developed by Grammont and colleagues (Sirveaux et al. 2004). While the biomechanical rationale for these has been explained (Kontaxis and Johnson 2006, DeWilde et al 2004, van der Helm 1998), there is little knowledge of the muscle activity required or the resulting joint and muscle forces. Furthermore, there is limited understanding of the optimum design configuration. For instance, while the Delta prosthesis uses a hemispherical component at the glenoid, the Bayley-Walker (B-W) prosthesis is a constrained design having a smaller diameter ball. Surgeons choosing shoulder implants to treat RC deficient patients need to understand how daily activity and muscle function affect fixation of implants in order to select the most appropriate design .

Fixed fulcrum TSR prostheses have a clear role in the management of shoulders in which the rotator cuff has failed. In one study (Soufali et al. 2005) pain relief was 81% after the first 2 years, reducing to 69% at 3.5 years post-operative (n=60). In an 11 year follow up study of the B-W prosthesis, it was found that, if loosening occurs, it does so in the majority of patients within the first 3 years (Bayley et al. 2005, Di Fabio et al. 2005). The B-W has a glenoid radiolucency incidence of 20% at a minimum 5 years post operative, compared with the previous Kessel device of 80% radiolucency (Bayley 2001).

1.2 Shoulder Model Validation

TSR design has evolved to an advanced stage with relatively poor knowledge of the biomechanics of the joint. Future, more advanced, designs are likely to require a more detailed understanding. One approach to improving knowledge of joint and muscle forces has been the development of sophisticated computer models such as the Newcastle shoulder model (Charlton and Johnson 2006).

However, while such models have been shown to be reasonably well validated at the hip using data from instrumented implants (Stansfield et al. 2003), no such validation has so far been shown at the shoulder, a more complex joint. Instrumented implants provide an ideal opportunity for this.

Although the forces acting at the prosthetic normal anatomy shoulder during activity are now becoming available (Bergmann et al. 2007), the way in which rotator cuff degeneration affects the glenohumeral joint force is completely unknown. This makes it impossible to predict functional outcomes for a range of rotator cuff deficiency and how this affects fixation of implants. The instrumented shoulder system reported here enables the measured forces to be correlated with a range of rotator cuff deficiency determined at and before surgery. Furthermore, analytical shoulder models customised for individual subjects' pathologies may be validated using the measured forces, potentially leading to further insights into the best rehabilitation protocols and implant loosening.

1.3 Glenoid Rim Stresses

A recent finite element (FE) study (Ahir et al. 2004) indicated that glenoid rim stresses were low using the B-W implant. A pilot study (in which strains were measured experimentally around the rim of sawbone scapulae implanted with either the standard B-W or a modified design for instrumenting the B-W glenoid component) has shown that in the modified component the strain energy density at the glenoid rim was significantly greater than for the current B-W design (Mordecai et al. 2005, 2007), thus better approximating load transfer in the normal anatomy. Thus the modified B-W component may prove to be an improved design for fixation.

2. DESIGN AIMS AND METHODOLOGY

The design of telemetric implant was based upon the existing reverse-anatomy B-W principle, in which a constrained ball and socket are interposed to displace the joint centre medially and thus increase the mechanical lever arm available to deltoid. The implant has tapering screw threads along its length which cut into the glenoid cortical and cancellous bone. The current telemetric study provided an opportunity for redesigning the implant to transfer more load onto the glenoid rim using a conical profile laterally and fewer screw threads medially in line with the findings of Mordecai et al (2005, 2007). This also provided a suitable cavity for housing the implant instrumentation. The aims of the study are to measure the 3 orthogonal forces F_x, F_y, F_z and torques M_x, M_y, M_z acting at the centre of the glenoid ball, fig. 1 (Taylor et al. 2004), during a range of daily activities and at several stages during rehabilitation up to 2 years postoperative.

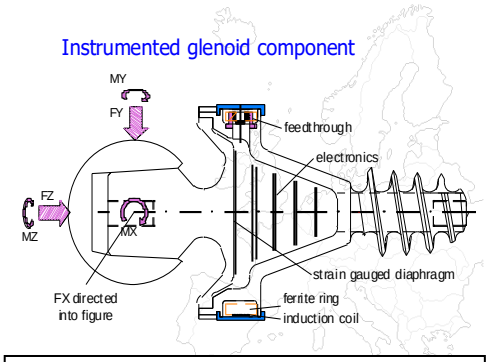

Fig 1: Implant force measurements

2.1 Implant Mechanical Design and FE Modelling

The modified implant design (hereinafter named the "conical" design) is shown in fig 2. In order to maintain as far as possible the medialised joint centre it was necessary to minimise the distance between the ball and glenoid bone surface. This was accomplished using an instrumented diaphragm as the load transducer to enable a short neck. In order to determine the optimum sites for the strain gauges, and the immunity to changes in the bone support conditions, a 3D finite element model was used. The 3D strain field at 12 radial sites on the inside of the diaphragm were determined from the model at several radii, for applied forces and torques along X, Y


Fig 2: Modified implant design

and Z axes. Three bone support conditions were simulated for each applied load and each strain site (full conical and screw support, partial (240deg arc) conical and full screw support, and no conical support (screw only). The data were analysed to determine sensitivities of each gauge to each applied force and torque. Design variables were the radius of the circle upon which the gauges were located and the angle of each gauge axis to the radial direction. Fig 3 shows the cross-sectional Von Mises stress variation during 1kN axial load, when the max stress was 86MPa.

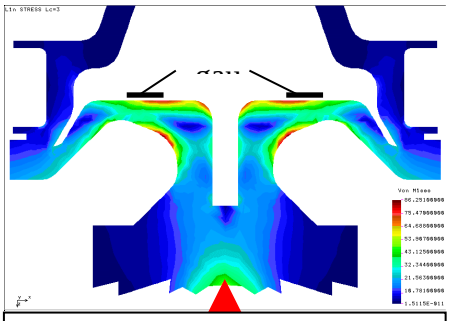

Fig 3: Von Mises stresses; 1kN

To provide access to the strain gauges and electronics during assembly, the implant was manufactured in 2 parts: the head/diaphragm and screw/cone (fig 4). These two parts were electron beam welded together after instrumentation. The cone/screw geometry was designed to transfer applied load to the cortical bone at the glenoid rim by a combination of axial and shear stress in the bone. The parallel sided screw was designed to secure the cone. The implanted cone is coated with hydroxyapatite for promoting osseointegration.

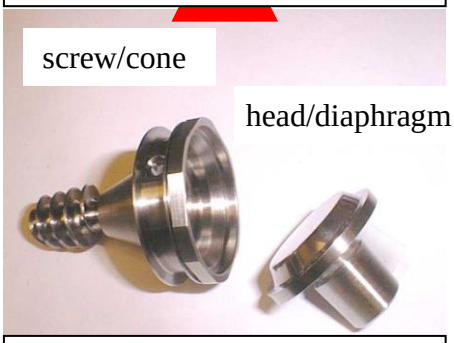

Fig 4: implant sections

2.2 Welding and Fatigue Testing

All electron beam weld parameters were tested for correct penetration and strength using prototype parts prior to final assembly. Welds were radiographed and sectioned to assess penetration and quality. The main weld between the head/diaphragm and screw/cone was 3mm deep. Two welded assemblies were fatigue tested to 5Mcycles with an applied peak load of 1kN axial and 500N shear force. Tufnel blocks were used to simulate the supporting glenoid bone. Two support conditions were simulated: full and partial conical support with full screw support. Implants were bathed in Ringer's solution. The coil assembly is electrically connected to the implant circuit via a feed-through. The feedthrough is welded into a holder which is then welded to the rim of the implant. This arrangement was also fatigue tested in a separate test with 4 such assemblies. Helium leak testing was carried out before and after the test to ascertain integrity of the hermetic seal.

2.3 Implant Electrical Instrumentation

The implant circuit consists of a high resolution, high bandwidth data sampler with on-board processor and data telemeter. Twelve thin film strain gauges of 10kΩ ± 0.1% are arranged at 30 deg intervals around a 10mm diameter on the inner flat surface of the diaphragm. Each gauge grid is aligned at 45 deg to its radial axis to provide maximum sensitivity to axial (Z axis) torque, which was found in the FE model to be the least sensitive component. Optimum gauge placements were determined from the FE analysis. Temperature compensation is provided by an LM35 temperature sensor die mounted on the diaphragm itself. The sensors are housed close to the amplifier and A-D converter, minimising electrical noise. Each strain channel is normally sampled at 100samples/sec and has a practical resolution of 0.25-0.5με. The implant circuitry was realised as a 4-layer flexible printed circuit, fig 5, folded and housed inside the cone.

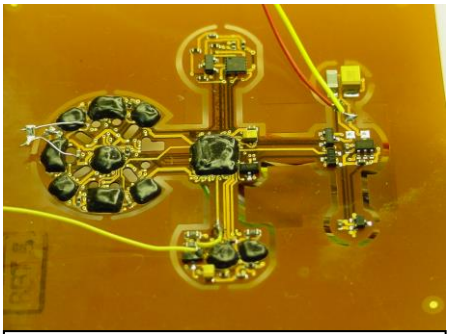

Fig 5: implant flexible circuit

2.4 Power Supply and Telemetry

Power is supplied to the implant and data telemetered via magnetic coupling between one external and one implanted coil, fig 2. (Taylor et al. 1997, 2001). Both coils form part of tuned circuits resonant at

1.216MHz. The master oscillator and drive unit are located in a small box carried by the patient, together with the microcontroller for controlling magnetic field strength and for receiving the serial telemetry signal. Telemetry is accomplished via amplitude modulation of the implant tuned circuit impedance reflected back to the primary.

2.5 Calibration Rig Design and Sensitivity Matrix

A calibration rig was custom built to enable many different combinations of the 6 measurands to be applied, over the following measurement ranges: F_x and F_y to 500N; F_z to 1.4kN, and torques M_x, M_y, and M_z to 5Nm (fig 6), (Taylor et al. 2006). Each axis was driven by stepper motors controlled by a LabView program. To apply axial force a stepper motor applied torque to a low-friction ball screw/spline, which created linear motion compressing a spring against the implant. Two smaller stepper motors simultaneously rotated a sprung-loaded gearwheel, and torque was thus applied to the stationary shaft by the springs. A degree of mechanical decoupling between axes was achieved using double universal joints on the X and Y axes which were partially constrained during axial compression to prevent buckling. Load cells were placed in line with each axis to measure any shear forces produced by adjacent axes as well as the desired axial forces and torques, and forces and couples acting in 3 planes were summed to determine the resultant 3 force and 3 torque components acting on the block and therefore the implant. The implant was housed on the machine bed. Temperature was controlled to 37degC.

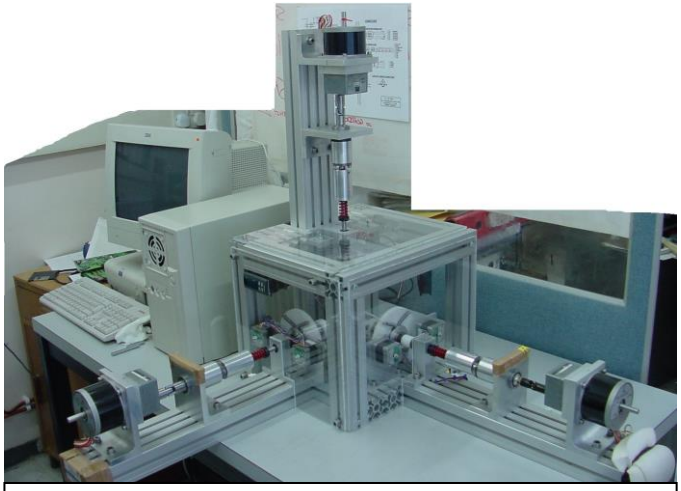

Fig 6: 3-axis force/torque calibration rig

The rig was operated by the LabView program which applied pre-set load combinations via the stepper motors. The in-line load cells provided feedback to adjust the loads according to the preset values, and a single load application took between 5-20 seconds. At each load, the implant strains were measured, telemetered, and captured. Several hundred load combinations were applied over the above force and torque ranges. Multiple linear regression was used to determine the sensitivity of each strain gauge channel to each applied load, producing a 12x6 calibration sensitivity matrix for each implant. This matrix was inverted using the pseudoinverse method. The resulting measurement sensitivity matrix for the instrumented device and the FE model were very similar, thus validating the method. Fig 7 plots the force sensitivities found from the FE model and from the calibration (arbitrary units), showing good overall agreement.

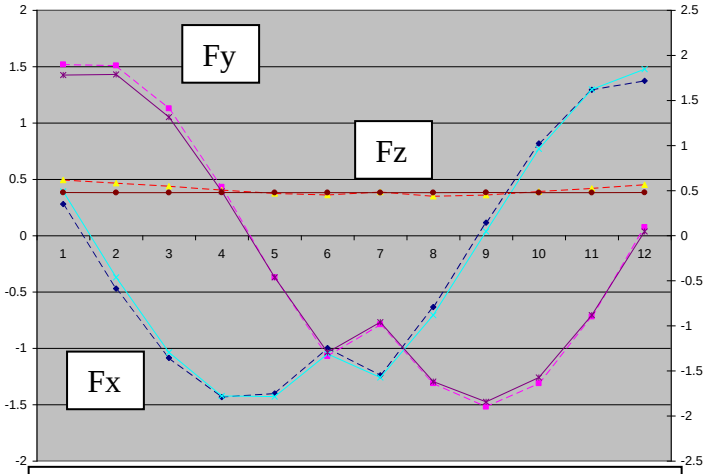

Fig 7: strain sensitivities for each channel in response to each applied Fx, Fy, Fz forces – solid lines: FE model; dotted lines: calibration

Two instrumented shoulder implants have so far been built ready for implantation. The degree of RC deficiency will be determined by MRI and during surgery. The subjects will attend a motion analysis laboratory during several postoperative sessions, when joint kinematics and *in vivo* forces will be measured simultaneously, during a range of activities. Further instrumented prostheses are being prepared for implantation.

SUMMARY

An instrumented reverse-anatomy shoulder implant has been designed and built for studying the relationship between joint forces and rotator cuff deficiency during activity. Three forces and moments are measured. The implant is powered and interrogated inductively. A 3D finite element model was used to determine optimum strain gauge locations. Two instrumented implants have so far been built; several more are in preparation. Calibration and FE-predicted sensitivities of strains to applied loads are in good agreement.

ACKNOWLEDGEMENT

This work was funded by the Arthritis Research Campaign.

REFERENCES

Ahir SP, Walker PS, Squire-Taylor CJ, Blunn GW, Bayley JI. Analysis of glenoid fixation for a reversed anatomy fixed-fulcrum shoulder replacement. J Biomech. 2004 Nov; **37**(11):1699-708.

Bayley JIL. Symposium on Shoulder Replacement in Complex Problems, RJAH Oswestry, 20 Sept 2001.

Bayley I. Shoulder replacement in rotator cuff deficient shoulders with arthritis. Wrightington International Arthroplasty Symposium, Manchester, July 2005.

Bergmann G, Graichen F, Bender A, Kaab M, Rohlmann A, Westerhoff P. In vivo glenohumeral contact forces - measurements in the first patient 7 months postoperatively. J Biomech. 2007; **40**(10): 2139-49.

Charlton IW, Johnson GR. A model for the prediction of the forces at the glenohumeral joint. Proc Inst Mech Eng [H]. 2006 Nov; 220(8):801-12.

De Wilde LF, Audenaert EA, Berghs BM. Shoulder prostheses treating cuff tear arthropathy: a comparative biomechanical study. J Orthop Res. 2004 Nov; **22**(6):1222-30.

Di Fabio S, Malone A, Calvert P, Lambert S, Bayley I. An analysis of failures in primary shoulder arthroplasty (PSA): predictable, therefore avoidable, consequences. JBJS Proc, Suppl. II, **87-B**, p163, 2005.

Kontaxis, A. Johnson G.R. (2006) Reverse anatomy shoulder prosthesis. a solution for severe rotator cuff tear. Proceedings of International Conference on Computer Methods in Biomechanics and Biomedical Engineering, Antibes, France.

Mordecai SC, Taylor SJG, Lambert S, Bayley JIL, Meswania JM, Blunn GW. Experimental strain analysis for an improved shoulder implant fixation; BOA, Birmingham, September 2005.

Mordecai SC, Lambert S, Bayley JIL, Blunn GW, Meswania JM, Taylor SJG. Experimental glenoid strain analysis for an improved reverse anatomy shoulder implant fixation. Submitted to J.Shoulder&Elbow Surg.

Sirveaux F, Favard L, Oudet D, Huquet D, Walch G, Mole D. Grammont inverted total shoulder arthroplasty in the treatment of glenohumeral osteoarthritis with massive rupture of the cuff. Results of a multicentre study of 80 shoulders. J Bone Joint Surg Br. 2004 Apr; **86**(3):388-95.

Soufali P, Malone A, Calvert P, Lambert S, Bayley I. Fixed-fulcrum total shoulder arthroplasty (FFTSA) for rotator cuff deficient shoulder with and without arthritis. JBJS Proc, Suppl. II, **87-B**, p163, 2005.

Stansfield BW, Nicol AC, Paul JP, Kelly IG, Graichen F, Bergmann G. Direct comparison of calculated hip joint contact forces with those measured using instrumented implants. An evaluation of a three-dimensional mathematical model of the lower limb. J Biomech. 2003 Jul; **36**(7):929-36.

Taylor SJG, Perry JS, Meswania JM, Donaldson N, Cannon SR, Walker PS. Telemetry of forces from proximal femoral replacements and relevance to fixation. J. Biomechanics **30** (3): 225-234, 1997.

Taylor SJG, Walker PS. Forces and moments telemetered from two distal femoral replacements during various activities. J Biomechanics **34**, No.7, pp839-848, 2001.

Taylor SJG, Meswania JM, Rodríguez-Arias J, Calle R, Bayley IL, Blunn GW. An instrumented implant and calibration technique for measurement of glenohumeral joint forces *in vivo*. European Society of Biomechanics, s'Hertogenbosch, July 2004.

Taylor SJG, Cuenca D, Blunn GW. Calibration technique for a 6 DOF force-measuring telemetric shoulder prosthesis. World Congress of Biomechanics, Munich, July 2006.

van der Helm FCT. The 'Reversed' glenohumeral endoprosthesis: The role of the rotator cuff muscles for stability and strength. 11th Conference of the ESB, July 8-11, 1998, Toulouse, France.